



HAL
open science

The BF4 and p71 antenna mutants from *Chlamydomonas reinhardtii*

Sandrine Bujaldon, Natsumi Kodama, Mithun Kumar Rathod, Nicolas Tourasse, Shin-Ichiro Ozawa, Julien Selles, Olivier Vallon, Yuichiro Takahashi, Francis-André Wollman

► **To cite this version:**

Sandrine Bujaldon, Natsumi Kodama, Mithun Kumar Rathod, Nicolas Tourasse, Shin-Ichiro Ozawa, et al.. The BF4 and p71 antenna mutants from *Chlamydomonas reinhardtii*. *Biochimica et Biophysica Acta (BBA) - Reviews on Bioenergetics*, 2019, 10.1016/j.bbabi.2019.148085 . hal-02880063

HAL Id: hal-02880063

<https://hal.sorbonne-universite.fr/hal-02880063>

Submitted on 24 Jun 2020

HAL is a multi-disciplinary open access archive for the deposit and dissemination of scientific research documents, whether they are published or not. The documents may come from teaching and research institutions in France or abroad, or from public or private research centers.

L'archive ouverte pluridisciplinaire **HAL**, est destinée au dépôt et à la diffusion de documents scientifiques de niveau recherche, publiés ou non, émanant des établissements d'enseignement et de recherche français ou étrangers, des laboratoires publics ou privés.

Title: The BF4 and *p71* antenna mutants from *Chlamydomonas reinhardtii*

Author names: Sandrine Bujaldon¹, Natsumi Kodama², Mithun Kumar Rathod², Nicolas Tourasse¹, Shin-Ichiro Ozawa², Julien Sellés¹, Olivier Vallon¹, Yuichiro Takahashi^{2*} and Francis-André Wollman^{1*}

Affiliations:

¹UMR7141 CNRS-Sorbonne Université, Institut de Biologie Physico-Chimique, Paris, 75005, France

²Research Institute for Interdisciplinary Science, Okayama University, Okayama, 700-8530, Japan

***Corresponding authors:** taka@cc.okayama-u.ac.jp ; wollman@ibpc.fr

Highlights:

- The BF4 mutant was characterized as defective in the insertase Alb3.1
- The p71 mutant was characterized as defective in cpSRP43
- cpSRP route accounts for biogenesis of 80% of LHCPs
- 20% LHCP may use an alternative biogenesis pathway

Abstract

Two pale green mutants of the green alga *Chlamydomonas reinhardtii*, which have been used over the years in many photosynthesis studies, the BF4 and *p71* mutants, were characterized and their mutated gene identified in the nuclear genome. The BF4 mutant is defective in the insertase Alb3.1 whereas *p71* is defective in cpSRP43. The two mutants showed strikingly similar deficiencies in most of the peripheral antenna proteins associated with either photosystem I or photosystem 2. As a result the two photosystems have a reduced antenna size with photosystem 2 being the most affected. Still up to 20 % of the antenna proteins remain in these strains, with the heterodimer Lhca5/Lhca6 showing a lower sensitivity to these mutations. We discuss these phenotypes in light of those of other allelic mutants that have been described in the literature and suggest that even though the cpSRP route serves as the main biogenesis pathway for antenna proteins, there should be an escape pathway which remains to be genetically identified.

Keywords: *Chlamydomonas*, photosynthesis, antenna, light harvesting complex, cpSRP, ALB3.

1. Introduction

The peripheral antenna proteins, hereafter referred to as Light-Harvesting Chlorophyll Protein (LHCP), accommodate chlorophyll *a* (Chl *a*) and chlorophyll *b* (Chl *b*) molecules which increase the light-harvesting capacity of each photosystem in green algae and vascular plants. They are encoded in the nucleus by two multigenic families, the *Lhca* (for PSI) and *Lhcb* (for PSII) genes. In the unicellular alga *Chlamydomonas reinhardtii*, the *Lhca* proteins associated with the PSI core complex are encoded by nine genes. One copy of *Lhca2-9* and two copies of *Lhca1* are bound to the PSI core [1, 2]. The major *Lhcb* proteins are encoded by nine genes (Type I: *LhcbM3/4/6/8/9*; Type II: *LhcbM5*; Type III: *LhcbM2/7*; Type IV: *LhcbM1*) while minor *Lhcb* proteins (CP26 and CP29) are coded for by the *Lhcb4* and *Lhcb5* genes, respectively. These LHCP proteins mainly transfer light energy to PSII core complexes, although some of these can migrate to the PSI membrane domains where they transfer their light excitation to the PSI cores upon a regulation process known as the State Transition process [3]. Besides these constitutive antenna polypeptides, there are two antenna-related proteins in *C. reinhardtii*, the *LhcSR* proteins (light-harvesting complex stress-related), which participate in photoprotection, by dissipating as heat the excess light energy absorbed by the antenna proteins [4]: *LhcSR1* which is constitutively expressed and *LhcSR3*, encoded by the 2 *LhcSR3.1/3.2* genes, which is expressed under high-light.

The LHCP mRNAs are translated in the cytosol into pre-apoproteins which are translocated through the chloroplast envelope by the TOC/TIC translocon before being processed to their mature form and inserted, as holoproteins folded with their pigment complement, in the thylakoid membranes. Several biogenesis factors are required for completion of the LHCP journey from the nucleo-cytosol to the thylakoid membranes (for reviews see [5, 6]). In *Chlamydomonas*, LHCP translation is controlled by the NAB1 protein, which is a repressor under redox control [7]. The release of pre-apoLHCP proteins from the translocon requires the LTD protein [8], which has a bias towards the PSI antenna apoproteins [9]. LTD hands them to the SRP complex comprised of two subunits cpSRP43 and cpSRP54. The LHCP-SRP complex is then targeted across the stroma to the thylakoid membranes where it docks to cpFtsY, the cpSRP complex receptor [6]. While cpFtsY interacts with cpSRP54 via their homologous GTPase domains, cpSRP43 and Alb3 interact directly via their C-terminal domains. Alb3 inserts the apoproteins into the membrane bilayer, concomitant with Chl association. It is of note that Alb3 interacts with the SecYE translocon, even though the latter is not responsible for LHCP integration. The existence of an alternative - SRP-independent - biogenesis pathway has been discussed several times [10, 11], in light of the observation that a double mutant from *Arabidopsis*, fully lacking cpSRP54 and cpSRP43, still accumulates peripheral antenna proteins in mature leaves [12]. It could rely on an apo- to holo- LHCP protein conversion occurring at the inner envelop membrane which, by membrane budding, would generate vesicle trafficking towards the thylakoids where the LHC proteins would insert by membrane fusion with these vesicles [13].

Chlamydomonas has been extensively used for in vivo spectroscopic studies of photosynthesis owing to its small size and amenability to genetic studies. Time-resolved absorption changes however are hampered by chlorophyll absorption in the blue and red region of the spectrum. Two mutants, BF4 and *p71*, which showed a marked decrease in chlorophyll content, proved useful for such spectroscopic studies due to their deficiency in peripheral antenna proteins [14-16]. In addition, the BF4 mutant has been instrumental in the original isolation of highly active PSII core preparations [17, 18] and in the identification of antenna proteins in freeze-fractured thylakoid membranes [19]. Since neither of these

two mutants had been characterized so far at the genetic level, we set out to identify the mutations responsible for their decreased antenna content. We provide a detailed characterization of the mutant phenotypes in comparison with antenna mutants from *C. reinhardtii* previously characterized by other groups.

2. Material and Methods

2.1. Strains and growth conditions

Wild type and mutant strains of *Chlamydomonas reinhardtii* were grown mixotrophically at 25°C in Tris-acetate-phosphate (TAP) medium, pH 7.2 [20] on a rotary shaker (150 rpm) under continuous light (5 or 50 $\mu\text{mol photons m}^{-2} \text{s}^{-1}$), unless otherwise indicated. Before being further characterized, the BF4 [19, 21], *p71* [22], *ac29-3* [23] mutants were backcrossed to our 137c-derived reference strains, either WT.T222 mating type (mt) + or WTS24 mt-, resp. CC-5101 and CC-5100 at the Chlamydomonas Resource Center, <https://www.chlamycollection.org/>, which also provided *tla3*, CC-4473 [24].

2.2. Chlorophyll Content

Chlorophyll concentrations were determined following extraction of the pigments in methanol [25].

2.3. Analysis of Polypeptides

For protein analysis of thylakoid membrane, cells were centrifuged at 2 000 x g for 5 min and resuspended in 5 mL of 5 mM HEPES/KOH pH 7.5 containing 10 mM EDTA and 0.3 M sucrose and broken in a French pressure cell at 27.56 MPa (4000 lb/in²). Thylakoid membranes were recovered using a flotation procedure adapted from [26]. In brief, the broken cell suspension was placed on top of a 4mL 1.8 M sucrose cushion containing 5mM HEPES/KOH pH 7.5 and 10mM EDTA, and spun in a swinging bucket rotor at 160 000 x g for 1 h. Thylakoid membranes were collected at the interface between the two layers. They were then resuspended in 10 mL of 5 mM HEPES/KOH pH 7.5 containing 10 mM EDTA and centrifuged at 17 500 x g for 30 min. Protease inhibitors were added in all solutions just before the experiment (Phenylmethylsulfonyl fluoride; 200 μM , Benzamide; 1 mM, 6-aminocaproic acid; 5 mM) and all steps were carried out at 4°C.

The thylakoid membranes or total cellular proteins were solubilized in the presence of 2% SDS and 0.1 M dithiothreitol (DTT) at 100°C for 90 seconds and then separated by high-molarity Tris SDS-PAGE without urea [27] or with 8 M urea [28]. The separated polypeptides were electroblotted onto a nitrocellulose filter. Immunodetection was performed using antibodies against PSI, PSII, LHC subunits, LhcSR [29] and phosphothreonine (Cell Signaling Technology). Signals were visualized by enhanced chemiluminescence (ECL) and detected with an LAS-4000 mini luminescent image analyzer (FujiFilm, Japan). We used antibodies against nine LHCI (LHCA1-9) [1, 30] and against six LHCII (LHCII Types I-IV, CP26, and CP29) [31].

2.4. Isolation of chlorophyll proteins complexes

The thylakoid membranes (0.4 mg Chl mL⁻¹) were solubilized with 1% (w/v) β -DDM, and centrifuged to remove insolubilized materials. The resulting extracts were separated by sucrose

density gradient ultracentrifugation and the gradient was fractionated from the bottom as described previously [32].

2.5. Fluorescence Measurements

Fluorescence induction kinetics were performed at room temperature using a DeepGreen Fluorometer (JBeamBio) and a home-built fluorescence CCD camera recorder [33]. Maximum efficiency of photosystem II, F_V/F_M ($F_V = F_M - F_0$), was determined using dark-adapted cells. Maximum fluorescence (F_M) was measured either after a saturating pulse, or upon continuous illumination in the presence of 10 μ M 3-(3,4-dichlorophenyl)-1, 1-dimethylurea (DCMU).

For state transition experiments, cells were placed in oxidizing conditions to achieve state 1, either by an incubation for 20 min under vigorous stirring in the dark or upon illumination in the presence of the PSII inhibitor DCMU (10 μ M). State 2 was achieved in reducing conditions, by placing the cells in anoxia. To this end, glucose (20 mM) and glucose oxidase (2 mg/mL) were added to cultures in the dark for 20 min. Fluorescence induction kinetics were monitored after addition of 10 mM DCMU on a DeepGreen Fluorometer (JBeamBio).

77 K fluorescence emission spectra were measured with an in house built setup. Samples were immersed in liquid nitrogen and excited with a LED source (LS-450, Ocean Optics - blue LED, 450 nm). The emission spectra were recorded using a CCD spectrophotometer (QE6500, Ocean Optics).

2.6. Genomic DNA Preparation, Whole-Genome Sequencing, and Data Analysis

DNA from wild-type strain, *p71* and BF4 mutant strains was extracted with the DNeasy Plant Maxi Kit (Qiagen), according to the manufacturer's protocol, starting from 100 mL of stationary culture. DNA from strain BF4-F35 was sequenced at the Tufts University core facility using the Illumina TrueSeq nano DNA method (2x100 nt) on a HiSeq 2500 instrument. Reads were mapped onto the reference genome (Phytozome V5.5) and analyzed using SVMerge 1.1.r32 [34] and inGAP-sv 2.8.1 [35] to identify mutations. The candidate genes in the MT locus were examined using the IGV 2.0 viewer [36]. To localize the *p71* mutation, strain *p71.A4+* was crossed with the highly polymorphic strain S1-D2 (CC-2290) and 120 *p71* progeny (scored on their low fluorescence phenotype), selected from independent tetrads, were pooled and grown for DNA preparation and Illumina sequencing (GATC, Germany, 2x125 nt). SHOREmap [37] was used to plot the proportion of S1-D2 polymorphisms along the chromosomes. A region lacking S1-D2-derived polymorphisms was identified on chromosome 4 and examined for mutations.

2.7. Complementation/Transformation of *C. reinhardtii*

The *Alb3.1* gene was amplified from wild-type *Chlamydomonas* genomic DNA. Primers used for amplification of the genomic sequence annealed to regions 760 bp upstream of the ALB3.1 transcription start site (5'- GCGCCGAACCGTATCTGGGA -3') and 450 bp downstream of the 3' UTR (5'- GATGCTCCGGTCCGGAAGCAC -3').

The *SRP43* coding sequence (CDS) was amplified by RT-PCR from wild-type *Chlamydomonas* total RNA with primers used in [24].

For complementation, mutant cells were grown in TAP medium at $20 \mu\text{mol photons m}^{-2} \text{s}^{-1}$ to early exponential phase ($1 \times 10^6 \text{ cells mL}^{-1}$), collected by centrifugation at room temperature at 4000 rpm for 7 min, and the cell pellet was re-suspended in TAP medium containing 40 mM sucrose (ToS) to a final cell concentration of $1 \times 10^8 \text{ cells mL}^{-1}$. For each mutant, the PCR product ($\sim 500 \text{ ng}$) plus 40 μg salmon sperm DNA and 160 ng of the *AphVIII* gene, was incubated with corresponding mutant cells at 16°C for 20 min. The cells were electroporated at 1kV, 10 μF capacitance, then incubated at 16°C . After 30 min of incubation, cells were diluted in 5 mL of ToS medium. The electroporated cultures were incubated overnight under dim light ($5 \mu\text{mol photons m}^{-2} \text{s}^{-1}$) with gentle agitation, then spread on solid minimum medium containing $10 \mu\text{g}\cdot\text{mL}^{-1}$ paromomycin and $100 \mu\text{g}\cdot\text{mL}^{-1}$ ampicillin and placed under light ($100 \mu\text{mol photons m}^{-2} \text{s}^{-1}$). After two weeks of growth, only transformants harboring the introduced gene (*Alb3.1*) or CDS (*SRP43*) were dark green and high fluorescence.

2.8. Spectroscopic studies

Cells were harvested during exponential growth ($2 \times 10^6 \text{ cells/mL}$) and were resuspended at a concentration of $1 \times 10^7 \text{ cells/mL}$ in minimum medium. The cell suspension was then vigorously stirred in a 50 mL Erlenmeyer flask for 20 min in the dark at 350 rpm.

Electrochromic shift (ECS) spectra were measured with a spectrometer built in house based on two Optical Parametric Oscillators (OPO). 10% (w/v) Ficoll was added in order to prevent cell sedimentation during the measurements. Cells were injected in two horizontal closed cuvettes with an optical path of 2.5 mm. Actinic flashes (700 nm) were provided by the first OPO pumped by a Nd:YAG laser (532 nm, 10 ns). Absorption changes due to saturating flashes were then sampled at selected wavelength and at discrete times with nanosecond flashes provided by the second OPO pumped by a Nd:YAG laser (355 nm, 10 ns). More details about the setup can be found in [38].

Determination of the PSII/PSI ratio and PSI antenna size, was performed with a Joliot-Type Spectrophotometer (JTS-10, Bio-Logic, Grenoble, France). Saturating flashes were provided by a dye laser (640 nm) pumped by a second harmonic of an Nd:Yag laser (Minilite II, Continuum). The continuous light beam was provided by LEDs. Detecting flashes of ECS signals were at 520 nm and 546 nm using interference filters (10 nm full width at half-maximum). PSI+PSII and PSI charge separations were calculated from changes in the amplitude of the fast phase (100 μs) of the ECS signal (measured as the 520 nm minus 546 nm absorbance changes) upon excitation with a saturating laser flash in the presence or absence of the PSII inhibitors, DCMU (20 μM) and hydroxylamine (HA) (1 mM). PSII contribution was calculated from the difference in ECS amplitude at 100 μs between the two conditions. PSI antenna size was measured from the slope of the saturation curve for PSI charge separation, using an OD attenuation of the laser flash fired at 640 nm.

3. Results

Chlamydomonas mutants with decreased chlorophyll content per cell are easily identified by their pale green phenotype associated with a low fluorescence yield (Fig. 1A and Table 1). Most of these mutants fall in either of two categories, peripheral antenna mutants or chlorophyll biosynthesis mutants, the latter most often displaying a light-dependent phenotype. Mutants of chlorophyll biosynthesis may also be photosensitive because of the accumulation of chlorophyll biosynthesis intermediates. The BF4 and *p71* mutants rather belonged to the first category since they were not photosensitive and their pale green phenotype was observed in darkness as well as under dim or

moderate light for growth, independent of the mixotrophic or photoautotrophic light growth condition (Fig. 1B).

The BF4 mutant was originally isolated after UV mutagenesis by Bennoun [19] and shown to be deficient in most of the LHCP proteins [21]. Mutant *p71*, isolated after 5-fluorodeoxyuridin mutagenesis, was screened by Girard-Bascou as a low LHCP-containing mutant in order to provide the appropriate genetic background for in vivo spectroscopic studies of *Chlamydomonas* [22]. Table 1 shows that the two mutants displayed a much higher Chl *a/b* ratio - close to 8 - than that in the wild type - about 3 - and about a three to four time lower content in chlorophyll per cell. Whole cell preparations had a decreased content in LHCI and LHCI proteins (Fig. 1C).

Since neither of these mutants had been further characterized at the gene level, we undertook a molecular identification of their genetic lesion (see M&M for details). We previously had noticed in crosses between BF4 to other strains that its mutation was genetically linked to the mt+ locus (see sup Fig.1 for typical tetrads). We thus searched the mt region in the BF4 genome, for possible changes in the sequence of candidate genes. We found a G>A substitution that destroys the 5' splice site of intron 4 within the *Alb3.1* gene (Cre06.g251900), 95 kb away from the *FUS1* gene of the mt+ locus (Sup Fig. 2). The predicted retention of the intron replaces the last 176 residues of the ALB3.1 protein, which are highly conserved, by an unrelated 76 amino acid sequence, presumably leading to an inactive protein. To identify the mutation in *p71*, we crossed it to the S1-D2 strain whose genome is profuse in polymorphisms with respect to that of our laboratory strains [39]. The *p71* progeny showed no S1-D2 polymorphism towards the end of chromosome 4. We found that a TOC1 transposon was inserted between introns 6 and 7 of the *SRP43* gene (Cre04.g231026) in the *p71* mutant (Sup Fig. 2). To assess that these mutational events were actually responsible for a low antenna phenotype, we respectively transformed the BF4 and *p71* mutants with a PCR-amplified genomic sequence of *Alb3.1* and a cDNA for the coding sequence of *SRP43* (see M&M for details). The complemented strains indeed showed restoration of a dark green phenotype and a higher fluorescence yield similar to that in the wild type (Fig. 1A&B). In addition the chlorophyll content per cell and Chl *a/b* ratio were restored to their wild-type levels (Table 1) and the LHCP proteins also were restored to a wild-type level (Fig. 1C).

The BF4 mutant should then be allelic to another previously identified *Alb3.1* mutant, *ac29-3* [23], while *p71* should be allelic to another previously identified *cpSRP43* mutant, *tla3* [24]. Indeed, the BF4 and *ac29-3* mutants have similar characteristics (Fig. 1, Table 1 and sup Fig. 3). The *p71* mutant displays phenotypic properties resembling those of *tla3*, as originally described, but is markedly different from the *tla3* strain recovered from the *Chlamydomonas* stock center (<https://www.chlamycollection.org/>) which has a much milder pigment-deficient phenotype (Fig. 2 and Table 1). It is likely that the latter strain bears additional mutation(s), responsible for reversion of the original *tla3* phenotype.

Table 1 shows that the F_v/F_M ratio was about twice as low in the *Alb3.1* and *SRP43* mutants as in the wild type. This is indicative of a change in content and/or organization of the PSII chlorophyll-binding proteins in the mutants. We thus further investigated the functional changes in photosynthesis resulting from the altered LHCP biogenesis pathway in the BF4 and *p71* mutants. In order to estimate changes in PSII antenna size in the mutants, we measured the half time of the fluorescence rise in presence of DCMU, an inhibitor of electron transfer beyond PSII, under continuous illumination of dark-adapted algae. Since only one charge separation is elicited in such condition, $1/t_{1/2}$ is a proxy of the relative PSII antenna size [40]. The two mutants displayed a dramatic decrease in PSII antenna size,

down to only 13% of the wild type (Fig. 2A). To provide an estimation of the PSI antenna size, we used the ECS measurement of a PSI charge separation in absence of PSII contribution, once it is inhibited by a preillumination in presence of HA and DCMU (see M&M section). Since the two mutants are deficient in peripheral antennae which contribute Chl *b* and carotenoid probes to ECS [41, 42], we first established their ECS spectrum, as shown on Fig. 2B. When measured 100 ms after a saturating actinic flash, we observed a blue shift of the spectrum of the mutants, in the 500-540 nm region, likely due to their decreased content in Chl *b* as we reported earlier [30]. Using the 520-546 difference, which eliminates the other spectral contributions from cyt *b₆f* and plastocyanin in this spectral region, we measured the PSI antenna size in the mutants relative to that in the wild type as the change in slope of the saturation curve for the PSI-driven ECS signal produced by a laser flash of varying intensity. In *p71* and BF4 the PSI antenna size was respectively 55% and 64% that in the wild type (Fig. 2A). Using the same single turnover laser flash of saturating light intensity, we compared the ECS signal 100 μ s after the flash when both PSI and PSII are active versus the ECS signal when PSII was inhibited by HA and DCMU. The resulting PSII/PSI ratio was similar to that in the wild type for the *p71* mutant but was smaller, 80%, in the BF4 mutant. The latter decrease points to a possible contribution of the Alb3.1 insertase to PSII biogenesis, as previously proposed [23]. We therefore probed the PSII and PSI protein contents in the thylakoid membranes of the two mutants (Table 1 and Fig. 3A). We observed the same polypeptide profile in the two mutants: at the chlorophyll loading used, their amount in PSII proteins relative to cyt *f* was similar to that in the wild type, whereas PSI proteins appeared more abundant. This is consistent with the lower PSII to PSI protein ratio shown in Fig. 2A. It is of note that the BF4 allelic mutant *ac29-3* also showed this PSII deficiency relative to PSI to an even larger extent than BF4 (sup Fig. 3). As previously reported [21], the D2 doublet, which arises from the presence of a phosphorylated form of the *psbD* gene product [43], was absent in these two LHCP mutants (Fig. 3A).

We then assessed the ability of the mutants to undergo state transitions, a reorganization of the light harvesting antenna which involves the lateral redistribution of phosphorylated antenna proteins between PSII and PSI. The maximal fluorescence F_M reflects the proportion of antenna proteins associated with PSII in either oxidizing (state 1) or reducing (state 2) conditions. In the wild type (Fig. 2A), LHCP movement towards PSI in reducing conditions resulted in a \sim 40% decrease of F_M as compared to its level in oxidizing conditions. This process was fully abolished in both the BF4 and *p71* mutants, which argues for a loss of mobile antenna in these two strains. Still phosphorylated forms of Lhcb proteins could be detected in the mutants with an antibody against phosphothreonine, when they were placed in state 2 conditions (Fig. 3B). The protein phosphorylation patterns were identical in the two mutants but displayed significant changes with respect to that in the wild type. On the one hand a new phosphoprotein, labeled X in Fig 3B, was detected in position of LhcbM1-Type IV, which lacks the regular target threonine at its N-terminus and is not phosphorylated in the wild type [44]. On the other hand, phosphorylation of D2 was lacking, consistent with the D2 antibody labeling pattern on Fig 3A, and phosphorylation of CP26 and CP29 remained below detection. Thus the lack of state transitions in the mutant cannot be ascribed to a loss in their ability to undergo antenna protein phosphorylation but rather to the low amount or absence of some of these phosphoproteins.

We then looked at the ability of the two mutants to express the LhcSR1 and LhcSR3 proteins involved in photoprotection. In *Chlamydomonas* LhcSR3 displays both a phosphorylated and an unphosphorylated form, but the expression of the two LhcSR3 forms together with LhcSR1, requires the cells to be placed in phototrophic conditions under high light (500 μ E) for several hours [29]. Fig3C shows that the two mutants when placed in these experimental conditions, retained the same LhcSR

expression profile as the wild type but displayed a lower level of these proteins, about 20%, similar to the level of the other Lhc proteins in these mutants (see below).

We next probed the chlorophyll organization between the two photosystems in the mutants by recording their 77K fluorescence emission spectra (Fig. 4). A wild-type spectrum shows two major peaks at 685 nm and 712-720 nm that respectively correspond to fluorescence emission from the PSII and PSI cores [45]. The amplitude of the PSI and PSII emission peaks is in part determined by the number of chlorophyll that transfer their light excitation to the fluorescence emitters. Here the cells were placed in state 1 conditions [44], a physiological situation where the mobile LHCI antenna is retained with PSII. At 77K, PSII also contributes a 695 nm peak, the amplitude of which depends on the coalescence between the long wavelength edge of the major PSII peak and the short wavelength edge of the PSI emission peak. This is readily observed in the four panels of Fig. 4, where the wild-type and mutant spectra were normalized at 685 nm. The two mutant spectra had similar features with an unchanged PSII emission peak at 685 nm, a slight enrichment in short wavelength emission in the 670 nm region and a red shift in PSI emission, now peaking at 716 nm instead of 712 nm. Whereas the former change suggests an enhanced contribution from some poorly connected LHCI whose emission peaks at 682 nm [44], the latter change is likely to result from the loss of most LHCI antenna whose emission peaks at 707 nm, thus allowing a better resolution of the 716 nm emission of the PSI cores [45]. The *p71* spectrum showed a large enhancement of the PSI emission peak relative to that of PSII, which is consistent with the higher number of core antenna chlorophyll in PSI than in PSII. A somewhat similar change of more limited amplitude was observed in the BF4 mutant. All changes in the 77K fluorescence emission of the mutants, were reversed in the complemented strains, which regained almost wild-type characteristics.

To get a better insight into the changes in content of the various LHCP proteins which contribute to the complex organization of the PSI (LHCI) and PSII (LHCII) peripheral antennae, we performed immunoblotting experiments using a complete set of antibodies raised against each of the *lhca* and *lhcb* gene products (for the specificity of the antibodies against Lhca1-9, see supplemental data in [30]). When loading whole cell protein extracts at the same chlorophyll concentration, as shown on Fig. 5, the two mutants displayed an expected higher amount of PSI and PSII than in the wild type (Fig. 5A) due to the drop in the peripheral antennae content. Indeed most LHCI and LHCII proteins in the mutants stood well below their amount in the wild type (Fig. 5B, C, D).

These results are consistent with the marked decrease in the antenna size of PSI and PSII in the mutants, but they also show that the LHCI and LHCII proteins are not completely absent in the mutants (except Lhca4). Since LHCI proteins assemble with the PSI core to form the PSI-LHCI supercomplex while most LHCII proteins are loosely bound to the PSII core to form PSII-LHCII supercomplex, we attempted to estimate the amount of each LHCI and LHCII proteins on a per PSI or PSII basis. We thus performed another series of immunoblotting experiments where the two mutant strains and the wild type solubilized in SDS were loaded at similar PSI or PSII content (Fig. 6A and B). It is of note that the amount of three PSI core subunits, PsaG, PsaK, and PsaN, were somewhat decreased in the mutants (especially BF4). Because of their interfacial position within the PSI-LHCI supercomplex [1], their binding to the rest of the PSI cores may be loosened in the absence of the peripheral antenna complement. As expected, the amount of each LHCI proteins was significantly decreased ($\leq 25\%$ of wild-type levels) in the mutants. However we noted some significant differences between the various PSI antenna proteins, with a better preservation of Lhca5 and Lhca6 than the other Lhca proteins.

These immunoblots also revealed that the LHCII proteins were similarly decreased at $\leq 25\%$ of wild-type levels. It is of note that no major differences were observed at the antenna protein level between the two mutants, despite their distinct mutations targeting different steps in the antenna biogenesis pathway.

We subsequently separated chlorophyll-protein complexes from the thylakoid extracts solubilized with β -DDM by sucrose density gradient ultracentrifugation as shown in Fig. 7. Three major green bands were separated from WT extracts: A1 contained LHCII, A2 mostly PSII core, and A3 the PSI-LHCI supercomplex plus some PSII supercomplex. In contrast, the yellow A1 and very faint A3 occasionally observed in *p71* and BF4 contained only trace amounts of LHCII and PSI-LHCI proteins, respectively. A2 contained both PSI and PSII core proteins with little if any peripheral antenna proteins. This indicates that PSI and PSII cores in the mutants did not form stable supercomplexes with the remaining peripheral antennae proteins.

4. Discussion

The present molecular genetic analysis of the BF4 and *p71* mutants from *C. reinhardtii* showed that they were allelic to other biogenesis mutants, defective for the Alb3.1 insertase [23] and cpSRP43 [24], further supporting the contribution of the major cpSRP route for LHCP insertion in the thylakoid membranes.

Both BF4 and *p71* accumulated Chls at only 15-20% of wild-type level, and immunoblotting of their LHCPs revealed that these mutants indeed showed severely reduced LHCI and LHCII protein levels. Since the LHCPs are the major chlorophyll binding proteins in the thylakoid membranes and bind both Chl *a* and Chl *b* whereas the reaction centers bind only Chl *a*, the low chlorophyll content and high Chl *a/b* ratio in these mutants is readily explained by their decreased amount in peripheral antenna proteins. The drastic drop by about 85% in functional PSII antenna size in these mutants is consistent with a quasi-absence of peripheral antenna connected to the PSII cores. Indeed the latter house 35 Chl, which represents 15% of the PSII antenna in a wild type placed in State 1 (reviewed in [3]). The decrease in PSI antenna size in the mutants is less extensive, as predicted from the larger number of chlorophyll, 94 molecules, housed within the PSI cores, compared to the 129 chlorophyll housed in their peripheral antenna [2]. The larger decrease in PSII antenna size than in PSI antenna size in the two mutants readily explains their higher PSI 77K fluorescence emission peak relative to that of PSII. However the decrease in PSII functional antenna size is larger than expected from the 25% remaining LHCII proteins in the mutants. This may explain why the mutants showed a marked drop in F_v/F_M and an enrichment in the short wavelength side of the PSII emission peak at 77K. The two latter observations indeed suggest that there are LHCII proteins which do not bind to PSII cores in the mutants. They would then contribute to basal fluorescence (F_0) at room temperature and emit fluorescence at shorter wavelength than PSII reaction center at 77K. The position of LHCII trimers within the PSII supercomplex shows that CP29 and CP26 control the interaction between LHCII/PSII cores [46, 47]. Their quasi-absence in the mutants should then prevent the association of the remaining LHCII with the cores. Based on the number of Chl in the core PSI and LHCI, a complete loss of the latter should lead to a remaining PSI antenna size of 44% that of the wild type. However, the functional antenna size that in the mutants was about $\sim 60\%$. The difference may be due to the remaining LHCI, but also to the association of a fraction of the remaining LHCII.

Consistent with the lack of interaction between the PSII cores and the ~25% LHCII remaining in the mutants was their complete loss of ability to perform state transitions, despite detection of phospho-LHCII in state 2 conditions. However the complete loss in antenna reorganization between unbound-LHCII and PSI upon LHC phosphorylation may result from the quasi-absence of CP29 and CP26 in the mutant as well as of the phospho-X extra band, possibly LhcbM1-Type IV, which may hamper antenna association with PSI. It is of note that the polypeptide patterns of the BF4 and *p71* mutant thylakoid membranes also lacked the upper PsbD band (D2.1) detected in the wild type which appears post-translationally and is due to phosphorylation of D2 at Thr2 [48]. This suggest that the kinase targeting D2 requires antenna proteins to recognize its substrate possibly through a phosphotransferase process between LHCII and D2 [49].

It is of note that the amounts of each LHCP protein - nine LHCI and six LHCII proteins - in the two mutants, is close to 25% of the wild-type content on a per-Chl basis. This suggests that the assembly of peripheral antenna proteins was not completely blocked and might occur, albeit at a lower rate, through an alternative route, possibly based on vesicle trafficking [13]. In addition this drop was less severe for Lhca5-6 than for Lhca1-2-3-4-7-8-9, indicating that the absence of Alb3.1 and cpSRP43 did not similarly impair the accumulation of each LHCI protein. In an attempt to rationalize these cpSRP-independent accumulation of LHCPs we investigated their sequence properties in the L18 domain which has been shown to be critical for using the cpSRP biogenesis route [50-52]. The primary sequence of all LHCPs contains two DPLG motifs for lutein binding [53]. It is the second motif, embedded within the L18 domain, VDPLYGGSFDPGLGLADD, located between helix C and helix B, which has been implicated in the interaction with cpSRP proteins. The canonical L18 domain could be identified in all LHCPs from *Chlamydomonas* albeit with a different degree of conservation (sup Fig. 4). The whole L18 domain was more conserved among Lhcb than Lhca proteins. The L18 domain in Lhcb4 (CP29) was the most divergent within the PSII peripheral antenna proteins whereas Lhca1 was the closest to Lhcb proteins, with Lhca2 and Lhca9 being the most divergent. A fully preserved DPLG motif was found in all LhcbM proteins whether of Type I, II III or IV, in Lhcb5 (CP26), LhcSR proteins and in Lhca1 and Lhca8. This motif bore one substitution in Lhcb4 (CP29) as well as in all other Lhca except for Lhca3 and Lhca6 which displayed three substitutions in this motif, keeping only L and P respectively (sup Fig. 4). Lhca6 accumulation was less sensitive than other Lhca proteins to the present mutations in the SRP-dependent pathway, but that of Lhca3 was as compromised as that of other Lhca proteins. Among all sequence divergence/conservation in the L18 domain and DPLG motif, only its absence in Lhca6 was consistent with a lower dependence on the SRP-biogenesis pathway. Lhca5 and Lhca6 form a hetero-dimer in the PSI supercomplex [2]. Since Lhca5 which keeps a bona fide DPLG motif accumulated as did Lhca6, we hypothesized that it is stabilized by its hetero-dimerization with Lhca6, incorporated in the membrane through an SRP-independent pathway. However, we are bound to conclude that the above sequence comparison did not allow us to draw a non-ambiguous correlation between the DPLG motif in the L18 domain and a possible escape from the cpSRP biogenesis pathway.

We next looked whether the supramolecular organization of the PSI-LHCI supercomplex [1, 2] could provide some structural basis for a better accumulation of Lhca5 and Lhca6 in the BF4 and *p71* mutants. Contrarily to what one could expect, these two subunits stand at the periphery of the protein complex, bound onto Lhca3 and Lhca7, with no direct interaction with the PSI cores. Still, the PSI antenna size in the mutants being larger (55% and 64%) than expected if only the PSI cores remained (44%), it is likely that the Lhca5/6 oligomer associates with the PSI cores and contributes a peripheral PSI antenna in the mutants. This PSI-LHCI association however should be much loosen in the mutants

as compared with that in the wild type since the relative stoichiometry of the Lhca subunits is deeply modified due to the excess content in Lhca5 and Lhca6. Indeed, it hardly resisted detergent solubilization and sucrose gradient centrifugation, as shown by the migration of most of the PSI complexes away from the A3 position in the wild type to the A2 position in the mutants, where stand the PSI cores without their peripheral antenna complement. Consistent with the lack of LHCII/PSII core interactions in the BF4 and *p71* mutants that we discussed above, PSII-LHCII supercomplexes also were absent in the mutants upon sucrose gradient centrifugation of solubilized thylakoids, a situation similar to what had been reported for the *tla3* and *ac29-3* mutants [24, 54].

A comparison with the main phenotypic traits of *ac29-3* and *tla3* mutants which are allelic to BF4 and *p71* [23, 24] points to several noticeable differences. The PSII antenna size in *tla3* was much larger than what we observed in *p71*, 42% versus 15% whereas the PSI antenna size was reduced to about the same extent (50%) in the two mutants. It had been argued previously that Alb3.1 contributes to the biogenesis of PSII, leading to a marked deficiency in PSII in the *ac29-3* mutant [23]. The BF4 mutant also showed a somewhat diminished content in PSII relative to PSI but its amplitude of about 20% was rather limited as compared to the previous report for *ac29-3* -from 50% to 90% depending on the growth conditions. Indeed when grown in similar light conditions, we observed a larger PSII deficiency in *ac29-3* (sup Fig. 3). The contrast between previous reports and the present study thus may be due to differences in genetic background between the mutant strains.

We observed a similar decrease in the PSII/PSI protein content in the *p71* mutant as in BF4 which, however, was not accompanied by a decrease in their functional ratio. This intriguing feature of *p71* suggests that a small fraction of PSI assembled in this mutant, less than 20%, would not undergo a stable charge separation, which is the functional event we measured by ECS. That some peripheral membrane subunits of PSI may require cpSRP43 for efficient assembly in a functional PSI protein complex remains to be investigated.

The previous and present studies concur in showing that Alb3.1 and cpSRP43 primarily contribute to the biogenesis of the peripheral antenna proteins. Still, about 25% of antenna proteins in these two mutants shows that the biogenesis process is not knocked out in either of these two strains. The point mutation at an exon/intron junction in the BF4 mutant, could result in a leaky phenotype allowing a limited expression of Alb3.1 and thereof the expression of low amounts of LHCP proteins. However, the residual antenna proteins detected in BF4 accumulate at the same level as in mutant *ac29-3* which carries a 3kb deletion in the *Alb3.1* gene. In addition the *p71* mutant, which carries a transposon insertion between introns 6 and 7 in the *cpSRP43* gene, also accumulates LHCP proteins to the same extent as in the Alb3-1 mutants. Last but not least, the Arabidopsis double mutant lacking the whole cpSRP complex, still accumulates antenna proteins in mature leaves [12]. These observations consistently argue for the existence of a cpSRP-independent route of low efficiency for the biogenesis of LHCP proteins. This pathway has escaped any genetic identification upon to now. Further genetic analysis of secondary mutations affecting Chl accumulation in the mutants of the SRP route may lead to interesting developments in this direction.

Acknowledgements

This work was supported by the 'Initiative d'Excellence' program from the French State (Grant 'DYNAMO', ANR-11-LABX-0011-01) and by JSPS KAKENHI Grant Number 16H06554. We thank Alberta Pinnola for providing the antibodies to LhcSR proteins.

References

- [1] S.-I. Ozawa, T. Bald, T. Onishi, H. Xue, T. Matsumura, R. Kubo, H. Takahashi, M. Hippler, Y. Takahashi, Configuration of Ten Light-Harvesting Chlorophyll *a/b* Complex I Subunits in *Chlamydomonas reinhardtii* Photosystem I, *Plant Physiology*, 178 (2018) 583-595.
- [2] M. Suga, S.-I. Ozawa, K. Yoshida-Motomura, F. Akita, N. Miyazaki, Y. Takahashi, Structure of the green algal photosystem I supercomplex with a decameric light-harvesting complex I, *Nature Plants*, (2019) in press.
- [3] W.J. Nawrocki, S. Santabarbara, L. Mosebach, F.-A. Wollman, F. Rappaport, State transitions redistribute rather than dissipate energy between the two photosystems in *Chlamydomonas*, *Nature Plants*, 2 (2016) 16031.
- [4] L. Wobbe, R. Bassi, O. Kruse, Multi-Level Light Capture Control in Plants and Green Algae, *Trends in Plant Science*, 21 (2016) 55-68.
- [5] L. Dall'Osto, M. Bressan, R. Bassi, Biogenesis of light harvesting proteins, *Biochimica et Biophysica Acta (BBA) - Bioenergetics*, 1847 (2015) 861-871.
- [6] D. Ziehe, B. Dünschede, D. Schünemann, Molecular mechanism of SRP-dependent light-harvesting protein transport to the thylakoid membrane in plants, *Photosynthesis Research*, (2018).
- [7] J.H. Mussnug, L. Wobbe, I. Elles, C. Claus, M. Hamilton, A. Fink, U. Kahmann, A. Kapazoglou, C.W. Mullineaux, M. Hippler, J. Nickelsen, P.J. Nixon, O. Kruse, NAB1 Is an RNA Binding Protein Involved in the Light-Regulated Differential Expression of the Light-Harvesting Antenna of *Chlamydomonas reinhardtii*, *The Plant Cell*, 17 (2005) 3409-3421.
- [8] M. Ouyang, X. Li, J. Ma, W. Chi, J. Xiao, M. Zou, F. Chen, C. Lu, L. Zhang, LTD is a protein required for sorting light-harvesting chlorophyll-binding proteins to the chloroplast SRP pathway, *Nature Communications*, 2 (2011) 277.
- [9] J. Jeong, K. Baek, J. Yu, H. Kirst, N. Betterle, W. Shin, S. Bae, A. Melis, E. Jin, Deletion of the chloroplast LTD protein impedes LHCI import and PSI-LHCI assembly in *Chlamydomonas reinhardtii*, *Journal of Experimental Botany*, 69 (2018) 1147-1158.
- [10] C.V. Richter, T. Bals, D. Schünemann, Component interactions, regulation and mechanisms of chloroplast signal recognition particle-dependent protein transport, *European Journal of Cell Biology*, 89 (2010) 965-973.
- [11] H. Kirst, A. Melis, The chloroplast signal recognition particle (CpSRP) pathway as a tool to minimize chlorophyll antenna size and maximize photosynthetic productivity, *Biotechnology Advances*, 32 (2014) 66-72.
- [12] P. Amin, D.A.C. Sy, M.L. Pilgrim, D.H. Parry, L. Nussaume, N.E. Hoffman, Arabidopsis Mutants Lacking the 43- and 54-Kilodalton Subunits of the Chloroplast Signal Recognition Particle Have Distinct Phenotypes, *Plant Physiology*, 121 (1999) 61-70.
- [13] J.K. Hooper, L.L. Eggink, M. Chen, Chlorophylls, ligands and assembly of light-harvesting complexes in chloroplasts, *Photosynthesis Research*, 94 (2007) 387-400.
- [14] G. Finazzi, F. Rappaport, A. Furia, M. Fleischmann, J.D. Rochaix, F. Zito, G. Forti, Involvement of state transitions in the switch between linear and cyclic electron flow in *Chlamydomonas reinhardtii*, *EMBO reports*, 3 (2002) 280-285.
- [15] Y. Li, A. van der Est, M.G. Lucas, V.M. Ramesh, F. Gu, A. Petrenko, S. Lin, A.N. Webber, F. Rappaport, K. Redding, Directing electron transfer within Photosystem I by breaking H-bonds in the cofactor branches, *Proceedings of the National Academy of Sciences*, 103 (2006) 2144-2149.

- [16] S. Santabarbara, B. Bullock, F. Rappaport, Kevin E. Redding, Controlling Electron Transfer between the Two Cofactor Chains of Photosystem I by the Redox State of One of Their Components, *Biophysical Journal*, 108 (2015) 1537-1547.
- [17] C. de Vitry, F.-A. Wollman, P. Delepelaire, Function of the polypeptides of the photosystem II reaction center in *Chlamydomonas reinhardtii*. Localization of the primary reactants, *Biochimica et Biophysica Acta (BBA) - Bioenergetics*, 767 (1984) 415-422.
- [18] C. de Vitry, C. Carles, B.A. Diner, Quantitation of plastoquinone-9 in photosystem II reaction center particles: Chemical identification of the primary quinone, electron acceptor Q_A, *FEBS Letters*, 196 (1986) 203-206.
- [19] J. Olive, F.-A. Wollman, P. Bennoun, M. Recouvreur, Ultrastructure of thylakoid membranes in *C. reinhardtii*: Evidence for variations in the partition coefficient of the light-harvesting complex-containing particles upon membrane fracture, *Archives of Biochemistry and Biophysics*, 208 (1981) 456-467.
- [20] E.H. Harris, *The Chlamydomonas sourcebook: introduction to Chlamydomonas and its laboratory use*, Academic Press, 2009.
- [21] C. de Vitry, F.-A. Wollman, Changes in phosphorylation of thylakoid membrane proteins in light-harvesting complex mutants from *Chlamydomonas reinhardtii*, *Biochimica et Biophysica Acta (BBA) - Bioenergetics*, 933 (1988) 444-449.
- [22] Y. Li, M.-G. Lucas, T. Konovalova, B. Abbott, F. MacMillan, A. Petrenko, V. Sivakumar, R. Wang, G. Hastings, F. Gu, J. van Tol, L.-C. Brunel, R. Timkovich, F. Rappaport, K. Redding, Mutation of the Putative Hydrogen-Bond Donor to P700 of Photosystem I, *Biochemistry*, 43 (2004) 12634-12647.
- [23] S. Bellaïfiore, P. Ferris, H. Naver, V. Göhre, J.-D. Rochaix, Loss of Albino3 Leads to the Specific Depletion of the Light-Harvesting System, *The Plant Cell*, 14 (2002) 2303-2314.
- [24] H. Kirst, J.G. Garcia-Cerdan, A. Zurbriggen, T. Ruehle, A. Melis, Truncated Photosystem Chlorophyll Antenna Size in the Green Microalga *Chlamydomonas reinhardtii* upon Deletion of the *TLA3-CpSRP43* Gene, *Plant Physiology*, 160 (2012) 2251-2260.
- [25] R.J. Porra, W.A. Thompson, P.E. Kriedemann, Determination of accurate extinction coefficients and simultaneous equations for assaying chlorophylls *a* and *b* extracted with four different solvents: verification of the concentration of chlorophyll standards by atomic absorption spectroscopy, *Biochimica et Biophysica Acta (BBA) - Bioenergetics*, 975 (1989) 384-394.
- [26] N.H. Chua, P. Bennoun, Thylakoid membrane polypeptides of *Chlamydomonas reinhardtii*: wild-type and mutant strains deficient in photosystem II reaction center, *Proceedings of the National Academy of Sciences of the United States of America*, 72 (1975) 2175-2179.
- [27] S.P. Fling, D.S. Gregerson, Peptide and protein molecular weight determination by electrophoresis using a high-molarity tris buffer system without urea, *Analytical Biochemistry*, 155 (1986) 83-88.
- [28] R.G. Piccioni, N.-H. Chua, P. Bennoun, A Nuclear Mutant of *Chlamydomonas reinhardtii* Defective in Photosynthetic Photophosphorylation, *European Journal of Biochemistry*, 117 (1981) 93-102.
- [29] G. Bonente, M. Ballottari, T.B. Truong, T. Morosinotto, T.K. Ahn, G.R. Fleming, K.K. Niyogi, R. Bassi, Analysis of LhcSR3, a protein essential for feedback de-excitation in the green alga *Chlamydomonas reinhardtii*, *PLoS Biol*, 9 (2011) e1000577-e1000577.
- [30] S. Bujaldon, N. Kodama, F. Rappaport, R. Subramanyam, C. de Vitry, Y. Takahashi, F.-A. Wollman, Functional Accumulation of Antenna Proteins in Chlorophyll *b*-Less Mutants of *Chlamydomonas reinhardtii*, *Molecular Plant*, 10 (2017) 115-130.
- [31] H. Takahashi, A. Okamuro, J. Minagawa, Y. Takahashi, Biochemical Characterization of Photosystem I-Associated Light-Harvesting Complexes I and II Isolated from State 2 Cells of *Chlamydomonas reinhardtii*, *Plant and Cell Physiology*, 55 (2014) 1437-1449.
- [32] I. Sugimoto, Y. Takahashi, Evidence That the PsbK Polypeptide Is Associated with the Photosystem II Core Antenna Complex CP43, *Journal of Biological Chemistry*, 278 (2003) 45004-45010.
- [33] X. Johnson, G. Vandystadt, S. Bujaldon, F.-A. Wollman, R. Dubois, P. Roussel, J. Alric, D. Béal, A new setup for in vivo fluorescence imaging of photosynthetic activity, *Photosynthesis Research*, 102 (2009) 85-93.

- [34] K. Wong, T.M. Keane, J. Stalker, D.J. Adams, Enhanced structural variant and breakpoint detection using SVMerge by integration of multiple detection methods and local assembly, *Genome Biology*, 11 (2010) R128.
- [35] J. Qi, F. Zhao, inGAP-sv: a novel scheme to identify and visualize structural variation from paired end mapping data, *Nucleic Acids Research*, 39 (2011) W567-W575.
- [36] H. Thorvaldsdóttir, J.T. Robinson, J.P. Mesirov, Integrative Genomics Viewer (IGV): high-performance genomics data visualization and exploration, *Briefings in Bioinformatics*, 14 (2012) 178-192.
- [37] K. Schneeberger, S. Ossowski, C. Lanz, T. Juul, A.H. Petersen, K.L. Nielsen, J.-E. Jørgensen, D. Weigel, S.U. Andersen, SHOREmap: simultaneous mapping and mutation identification by deep sequencing, *Nature Methods*, 6 (2009) 550.
- [38] D. Béal, F. Rappaport, P. Joliot, A new high-sensitivity 10-ns time-resolution spectrophotometric technique adapted to in vivo analysis of the photosynthetic apparatus, *Review of Scientific Instruments*, 70 (1999) 202-207.
- [39] C.H. Gross, L.P. Ranum, P.A. Lefebvre, Extensive restriction fragment length polymorphisms in a new isolate of *Chlamydomonas reinhardtii*, *Current genetics*, 13 (1988) 503-508.
- [40] F.-A. Wollman, J. Olive, P. Bennoun, M. Recouvreur, Organization of the photosystem II centers and their associated antennae in the thylakoid membranes: a comparative ultrastructural, biochemical, and biophysical study of *Chlamydomonas* wild type and mutants lacking in photosystem II reaction centers, *The Journal of Cell Biology*, 87 (1980) 728-735.
- [41] S. Schmidt, R. Reich, H.T. Witt, Electrochromism of chlorophylls and carotenoids in multilayers and in chloroplasts, *Naturwissenschaften*, 58 (1971) 414.
- [42] H.T. Witt, Energy conversion in the functional membrane of photosynthesis. Analysis by light pulse and electric pulse methods, *Biochimica et Biophysica Acta (BBA) - Reviews on Bioenergetics*, 505 (1979) 355-427.
- [43] P. Delepelaire, F.-A. Wollman, Correlations between fluorescence and phosphorylation changes in thylakoid membranes of *Chlamydomonas reinhardtii* in vivo: A kinetic analysis, *Biochimica et Biophysica Acta (BBA) - Bioenergetics*, 809 (1985) 277-283.
- [44] F.-A. Wollman, P. Delepelaire, Correlation between changes in light energy distribution and changes in thylakoid membrane polypeptide phosphorylation in *Chlamydomonas reinhardtii*, *The Journal of Cell Biology*, 98 (1984) 1-7.
- [45] F.-A. Wollman, P. Bennoun, A new chlorophyll-protein complex related to Photosystem I in *Chlamydomonas reinhardtii*, *Biochimica et Biophysica Acta (BBA) - Bioenergetics*, 680 (1982) 352-360.
- [46] X. Su, J. Ma, X. Wei, P. Cao, D. Zhu, W. Chang, Z. Liu, X. Zhang, M. Li, Structure and assembly mechanism of plant C₂S₂M₂-type PSII-LHCII supercomplex, *Science*, 357 (2017) 815-820.
- [47] B. Drop, M. Webber-Birungi, S.K.N. Yadav, A. Filipowicz-Szymanska, F. Fusetti, E.J. Boekema, R. Croce, Light-harvesting complex II (LHCII) and its supramolecular organization in *Chlamydomonas reinhardtii*, *Biochimica et Biophysica Acta (BBA) - Bioenergetics*, 1837 (2014) 63-72.
- [48] S.V. Bergner, M. Scholz, K. Trompelt, J. Barth, P. Gäbelein, J. Steinbeck, H. Xue, S. Clowez, G. Fucile, M. Goldschmidt-Clermont, C. Fufezan, M. Hippler, STATE TRANSITION7-Dependent Phosphorylation Is Modulated by Changing Environmental Conditions, and Its Absence Triggers Remodeling of Photosynthetic Protein Complexes, *Plant physiology*, 168 (2015) 615-634.
- [49] F.-A. Wollman, C. Lemaire, Phosphorylation processes interacting in vivo in the thylakoid membranes from *C. reinhardtii*, in: D. Hall, G. Grassi (Eds.) *Photocatalytic Production of Energy Rich Compounds*, Elsevier, Amsterdam, 1988, pp. 210-214.
- [50] J. DeLille, E.C. Peterson, T. Johnson, M. Moore, A. Kight, R. Henry, A novel precursor recognition element facilitates posttranslational binding to the signal recognition particle in chloroplasts, *Proceedings of the National Academy of Sciences*, 97 (2000) 1926-1931.
- [51] C.J. Tu, E.C. Peterson, R. Henry, N.E. Hoffman, The L18 Domain of Light-harvesting Chlorophyll Proteins Binds to Chloroplast Signal Recognition Particle 43, *Journal of Biological Chemistry*, 275 (2000) 13187-13190.

- [52] K.F. Stengel, I. Holdermann, P. Cain, C. Robinson, K. Wild, I. Sinning, Structural Basis for Specific Substrate Recognition by the Chloroplast Signal Recognition Particle Protein cpSRP43, *Science*, 321 (2008) 253-256.
- [53] T. Barros, W. Kühlbrandt, Crystallisation, structure and function of plant light-harvesting Complex II, *Biochimica et Biophysica Acta (BBA) - Bioenergetics*, 1787 (2009) 753-772.
- [54] F. Ossenbühl, V. Göhre, J. Meurer, A. Krieger-Liszkay, J.-D. Rochaix, L.A. Eichacker, Efficient Assembly of Photosystem II in *Chlamydomonas reinhardtii* Requires Alb3.1p, a Homolog of Arabidopsis ALBINO3, *The Plant Cell*, 16 (2004) 1790-1800.

Figures legend

Figure 1: Phenotypes of the LHCP mutants. (A) Maximal Fluorescence (F_M) of wild type (WT), *srp43* mutants (*p71* and *tla3*), *alb3.1* mutants (BF4 and *ac29-3*) and the rescued mutants (*p71-SRP43* and BF4-*ALB3.1*) grown onto solid TAP medium under moderate light (the color bar represents the fluorescence level) and (B) Growth patterns. Cultures were spotted on TAP or minimum medium (MIN) after 6 days under different light conditions, darkness (D), dim light (DL; $5 \mu\text{mol photons m}^{-2} \text{s}^{-1}$), moderate light (ML; $50 \mu\text{mol photons m}^{-2} \text{s}^{-1}$). (C) Immunoblots of whole-cell protein extracts (100% corresponding to $20 \mu\text{g}$ of chlorophyll) of wild type (WT), light-harvesting complex mutants (*p71* and BF4) and the complemented mutants grown in moderate light ($50 \mu\text{mol photons m}^{-2} \text{s}^{-1}$), probed with specific antibodies for LHCPs and tubulin as a loading control (proteins were separated by SDS-PAGE 12%).

Figure 2: Functional Photosystem II and Photosystem I relative antenna size, state transition, PSII/PSI ratio and Electrochromic shift spectra of the wild type (WT) and the LHCP mutants (*p71* and BF4) of *C. reinhardtii* grown photoautotrophically under moderate light ($50 \mu\text{mol photons m}^{-2} \text{s}^{-1}$). (A) Photosystem II and Photosystem I relative antenna size, Fluorescence quenching between state 1 and state 2 (R, reducing conditions analogous to state 2; O, oxidizing conditions analogous to state 1) and ratio PSII/PSI as measured by ECS (functional ratio) or by densitometric scanning of immunoblots (protein ratio with respect to wild type set as 1). PSII antenna size has been estimated from fluorescence rise kinetics to $F_M (1/t_{1/2})$ in the presence of DCMU (10^{-5} M) and PSI antenna size, estimated spectroscopically from the light-saturation curves of the ECS changes at (520 – 546) nm in the presence of PSII inhibitors (DCMU and hydroxylamine). (B) Electrochromic shift (ECS) spectra. The absorption change was measured 100 ms after the actinic flash hitting 100% of centers. All values represent means \pm SD ($n = 3 - 7$).

Figure 3: Protein Accumulation and Phosphorylation in thylakoids from LHCP mutants. Immunoblots of thylakoid membranes (100% corresponding to $20 \mu\text{g}$ of chlorophyll) from wild-type control (WT), *p71* and BF4 mutants grown in TAP under moderate light ($50 \mu\text{mol photons m}^{-2} \text{s}^{-1}$) (A), and then placed in anoxia (reducing conditions to achieve state 2) (B) or exposed to high light ($500 \mu\text{mol photons m}^{-2} \text{s}^{-1}$) in minimum medium for 4 h (C). Proteins were fractionated by electrophoresis on an 8 M urea 12-18% polyacrylamide gradient gel and probed with the antibodies as indicated: (A) PsaA/PsaD (subunits of Photosystem I); D1/D2 (PsbA/PsbD subunit of Photosystem II); CP47 (PsbB subunit of Photosystem II) and Cyt *f* (cytochrome *f*), (B) phosphothreonine (the identity of the phosphorylated proteins is indicated on the left), (C) LhcSR (LhcSR1, LhcSR3 and phosphorylated LhcSR3); (*npq4*; mutant lacking LhcSR3).

Figure 4: Low-temperature (77K) fluorescence emission spectra of cells in state 1 of wild type (WT), light-harvesting complex mutants (*p71* and BF4) and the complemented mutants grown in moderate light ($50 \mu\text{mol photons m}^{-2} \text{s}^{-1}$). All fluorescence emission spectra are normalized on PSII emission at 685 nm.

Figure 5: Accumulations of PSI, PSII, LHCI, and LHCI proteins in *p71*, BF4 and wild type, on a chlorophyll basis. WT (wild type), *p71* and BF4 cells were grown in TAP medium, and resuspended in buffer (50 mM Tris HCl pH 8.0, 20% (w/v) glycerol, 1 mM EDTA-NaOH pH 8.0). Cells at 0.1 (C) or 0.2 μg (A, B, and D) Chls were solubilized with 2% (w/v) SDS and 0.1 M DTT at 100°C for 1 min, and protein extracts were separated by SDS-PAGE, electroblotted onto a nitrocellulose filter, probed with specific

antibodies, and visualized by enhanced chemiluminescence. The filter was hybridized with antibodies against (A) PSI and PSII proteins (PsaA, PsaD, PsaF, PsaL, PsaK and PsbA), (B) LHCI proteins (Lhca1-9), (C) LHCII proteins (Type I, III, and IV) (D) LHCII proteins (CP26, CP29, and LHCII Type II). The arrowheads indicate the signals representing the actual antigen.

Figure 6: Accumulations of LHCI and LHCII proteins in *p71*, BF4 and wild type, on a reaction center basis. Cells were grown in TAP medium and resuspended in buffer (50 mM Tris HCl pH 8.0, 20% (w/v) glycerol, 1 mM EDTA-NaOH pH 8.0). Cells were solubilized with 2% (w/v) SDS and 0.1 M DTT at 100°C for 1 min, and protein extracts were separated by SDS-PAGE, electroblotted onto a nitrocellulose filter, probed with specific antibodies, and visualized by enhanced chemiluminescence. WT, wild type. The arrowhead indicates Lhca6. (A) Accumulation of PSI subunits and LHCI proteins on a PsaA basis. The nitrocellulose filter was hybridized with antibodies against PSI subunits (PsaA, PsaD, PsaF, PsaG, PsaH, PsaK, PsaL, and PsaN), LHCI (Lhca1-9). Relative loaded Chl amounts (%) are indicated on the top of lanes. (B) Accumulation of LHCII proteins on a PSII basis. The nitrocellulose filter was hybridized with antibodies against PSII (PsbA) and LHCII (CP26, CP29, LHCII Types I-IV). Relative loaded Chl amounts (%) are indicated on the top of lanes.

Figure 7: Separation of PSI, PSII, and LHCII complexes. (A) Thylakoid membranes of WT (wild type), *p71* and BF4 cells were solubilized with 0.8 % β -DDM and the extracts were separated by sucrose density gradient ultracentrifugation. A1, A2, and A3 represent LHCII, PSII core, and PSI-LHCI supercomplexes. (B) Polypeptides of A1, A2, and A3 were separated by SDS-PAGE and stained by Coomassie Brilliant Blue. Black asterisks: LHCII proteins, red asterisks: PSI proteins, and blue asterisks: PSII proteins.

Supplementary Figure 1: Fluorescence (F_M) image (A) and PCR mating type test (B) of 2 typical tetrads from a cross between WTS24, mt- and BF4, mt+. Note that the BF4 progeny which are blue spots in (A) are mt+ in (B).

Supplementary Figure 2: (A) Genomic sequence of the *Alb3.1* gene in WT and BF4. (B) The *SRP43* coding sequence (CDS) in WT and *p71*

Supplementary Figure 3: Comparative analysis of antenna protein content in BF4 and *ac29-3* mutants. WT (wild type), BF4, and *ac29-3* cells were grown in TAP medium and cells were suspended in buffer (50 mM Tris HCl pH 8.0, 20% (w/v) glycerol, 1 mM EDTA-NaOH pH 8.0). Cells were solubilized with 2% (w/v) SDS and 0.1 M DTT at 100°C for 1 min. Cell proteins were separated by SDS-PAGE on a PSI basis, electroblotted onto a nitrocellulose filter, probed with specific antibodies, and visualized by enhanced chemiluminescence. The arrowheads indicate the signals representing the actual proteins. The filter was hybridized with antibodies against PsaF, PsbA, LHCII Type I, III, and IV, Lhca2, Lhca5, Lhca6, and Lhca8. Relative loaded amount of chlorophylls (%) are indicated on the top of blots.

Supplementary Figure 4: Sequence alignment of L18 domain between LHC proteins from *Chlamydomonas reinhardtii*. Conserved L18 domain is highlighted in blue and the DPLG motif in red.

Table(s)

Table 1: Chlorophyll and fluorescence parameters of wild type (WT), *srp43* and *alb3.1* mutants and *p71-SRP43* and BF4-*ALB3.1* complemented mutants.

parameter		WT	<i>srp43</i> mutants		<i>alb3.1</i> mutants		Complemented strains	
			<i>p71</i>	<i>tla3</i>	BF4	<i>ac29-3</i>	<i>p71-SRP43</i>	BF4- <i>ALB3.1</i>
[Chl] ($\mu\text{g}/10^6$ cell)	DL	1.3 \pm 0.3	0.24 \pm 0.07	-	0.28 \pm 0.05	-	1.1 \pm 0.1	1.01 \pm 0.04
	ML	2.1 \pm 0.3	0.35 \pm 0.02	0.96 \pm 0.05	0.24 \pm 0.03	0.37 \pm 0.06	0.8 \pm 0.04	1.0 \pm 0.1
Chl a / Chl b	DL	2.9 \pm 0.2	8.2 \pm 0.2	-	8.4 \pm 0.8	-	3.2 \pm 0.1	3.5 \pm 0.1
	ML	3.1 \pm 0.1	6.9 \pm 0.4	6.2 \pm 0.1	9 \pm 2	12.7 \pm 0.3	4.1 \pm 0.2	3.2 \pm 0.1
F_M / Cell	DL	100%	8% \pm 3	-	8.1% \pm 0.5	-	71% \pm 2	79% \pm 3
	ML	100%	6.9% \pm 0.3	33.1% \pm 0.4	5% \pm 1	7.5% \pm 0.2	58% \pm 2	62% \pm 5
F_V / F_M	DL	0.75 \pm 0.01	0.35 \pm 0.02	-	0.35 \pm 0.06	-	0.70 \pm 0.01	0.68 \pm 0.04
	ML	0.74 \pm 0.02	0.33 \pm 0.03	0.52 \pm 0.01	0.35 \pm 0.01	0.31 \pm 0.02	0.74 \pm 0.01	0.64 \pm 0.06

Chlorophyll concentrations were determined according to [25]. Percentage was determined by comparison of the mutant with the wild type cells grown under the same light condition. Values represent means \pm SD (n= 3 – 7). DL, dim light (5 $\mu\text{mol photons m}^{-2} \text{s}^{-1}$); ML, moderate light (50 $\mu\text{mol photons m}^{-2} \text{s}^{-1}$).

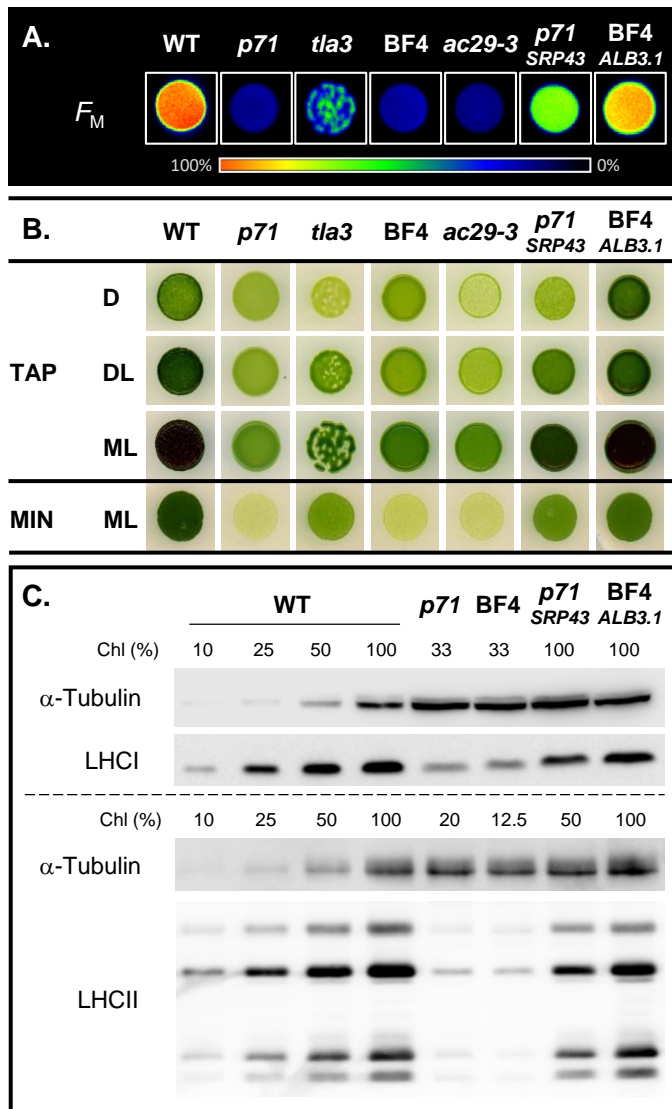


Figure 1: Phenotypes of the LHCP mutants.

(A) Maximal Fluorescence (F_M) of wild type (WT), *srp43* mutants (*p71* and *tla3*), *alb3.1* mutants (BF4 and *ac29-3*) and the rescued mutants (*p71-SRP43* and BF4-*ALB3.1*) grown onto solid TAP medium under moderate light (the color bar represents the fluorescence level) and (B) Growth patterns. Cultures were spotted on TAP or minimum medium (MIN) after 6 days under different light conditions, darkness (D), dim light (DL; 5 $\mu\text{mol photons m}^{-2} \text{s}^{-1}$), moderate light (ML; 50 $\mu\text{mol photons m}^{-2} \text{s}^{-1}$). (C) Immunoblots of whole-cell protein extracts (100% corresponding to 20 μg of chlorophyll) of wild type (WT), light-harvesting complex mutants (*p71* and BF4) and the complemented mutants grown in moderate light (50 $\mu\text{mol photons m}^{-2} \text{s}^{-1}$), probed with specific antibodies for LHCPs and tubulin as a loading control (proteins were separated by SDS-PAGE 12%).

A.

parameter	WT	<i>p71</i>	BF4
PSII $1/t_{1/2}$ fluorescence rise (DCMU)	1.0	0.13 ± 0.02	0.13 ± 0.02
PSI flash induced ECS DCMU+HA insensitive	1.0	0.55 ± 0.09	0.64 ± 0.01
$F_M(R) / F_M(O)$	$63\% \pm 3$	$100\% \pm 1$	$101\% \pm 2$
PSII/PSI functional ratio	1.03 ± 0.06	1.10 ± 0.05	0.8 ± 0.1
PSII/PSI protein ratio	1.0	0.7 ± 0.1	0.6 ± 0.1

B.

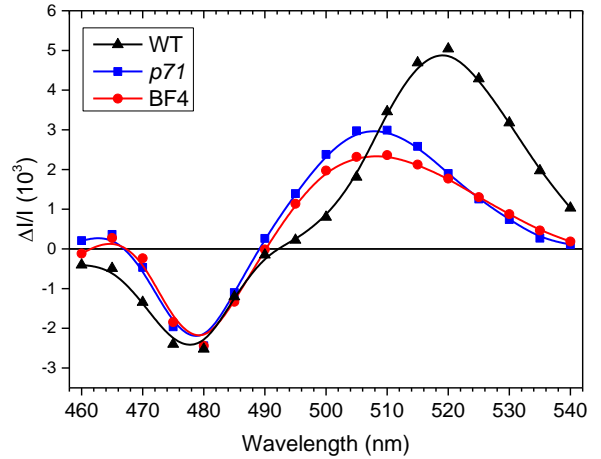


Figure 2: Functional Photosystem II and Photosystem I relative antenna size, state transition, PSII/PSI ratio and Electrochromic shift spectra of the wild type (WT) and the LHCP mutants (*p71* and BF4) of *C. reinhardtii* grown photoautotrophically under moderate light ($50 \mu\text{mol photons m}^{-2} \text{s}^{-1}$). (A) Photosystem II and Photosystem I relative antenna size, Fluorescence quenching between state 1 and state 2 (R, reducing conditions analogous to state 2; O, oxidizing conditions analogous to state 1) and ratio PSII/PSI as measured by ECS (functional ratio) or by densitometric scanning of immunoblots (protein ratio with respect to wild type set as 1). PSII antenna size has been estimated from fluorescence rise kinetics to $F_M(1/t_{1/2})$ in the presence of DCMU (10^{-5}M) and PSI antenna size, estimated spectroscopically from the light-saturation curves of the ECS changes at (520 – 546) nm in the presence of PSII inhibitors (DCMU and hydroxylamine). (B) Electrochromic shift (ECS) spectra. The absorption change was measured 100 ms after the actinic flash hitting 100% of centers. All values represent means \pm SD ($n = 3 - 7$).

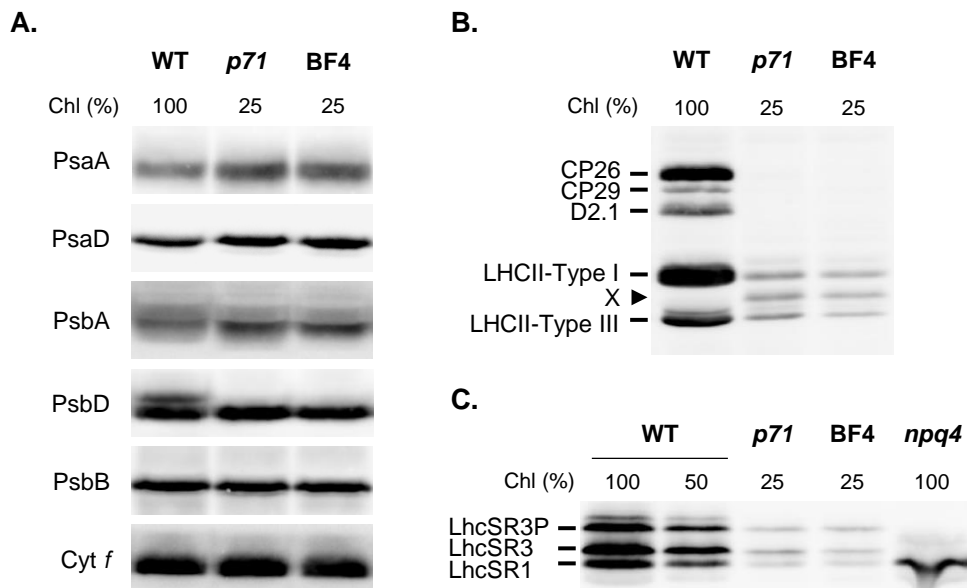


Figure 3: Protein Accumulation in thylakoids from LHCP mutants.

Immunoblots of thylakoid membranes (100% corresponding to 20 μg of chlorophyll) from wild-type control (WT), *p71* and BF4 mutants grown in TAP under moderate light (50 $\mu\text{mol photons m}^{-2} \text{s}^{-1}$) (A), and then placed in anoxia (reducing conditions to achieve state 2) (B) or exposed to high light (500 $\mu\text{mol photons m}^{-2} \text{s}^{-1}$) in minimum medium for 4 h (C). Proteins were fractionated by electrophoresis on an 8 M urea 12-18% polyacrylamide gradient gel and probed with the antibodies as indicated: (A) PsaA/PsaD (subunits of Photosystem I); D1/D2 (PsbA/PsbD subunit of Photosystem II); CP47 (PsbB subunit of Photosystem II) and Cyt *f* (cytochrome *f*), (B) phosphothreonine (the identity of the phosphorylated proteins is indicated on the left), (C) LhcSR (LhcSR1, LhcSR3 and phosphorylated LhcSR3); (*npq4*; mutant lacking LhcSR3).

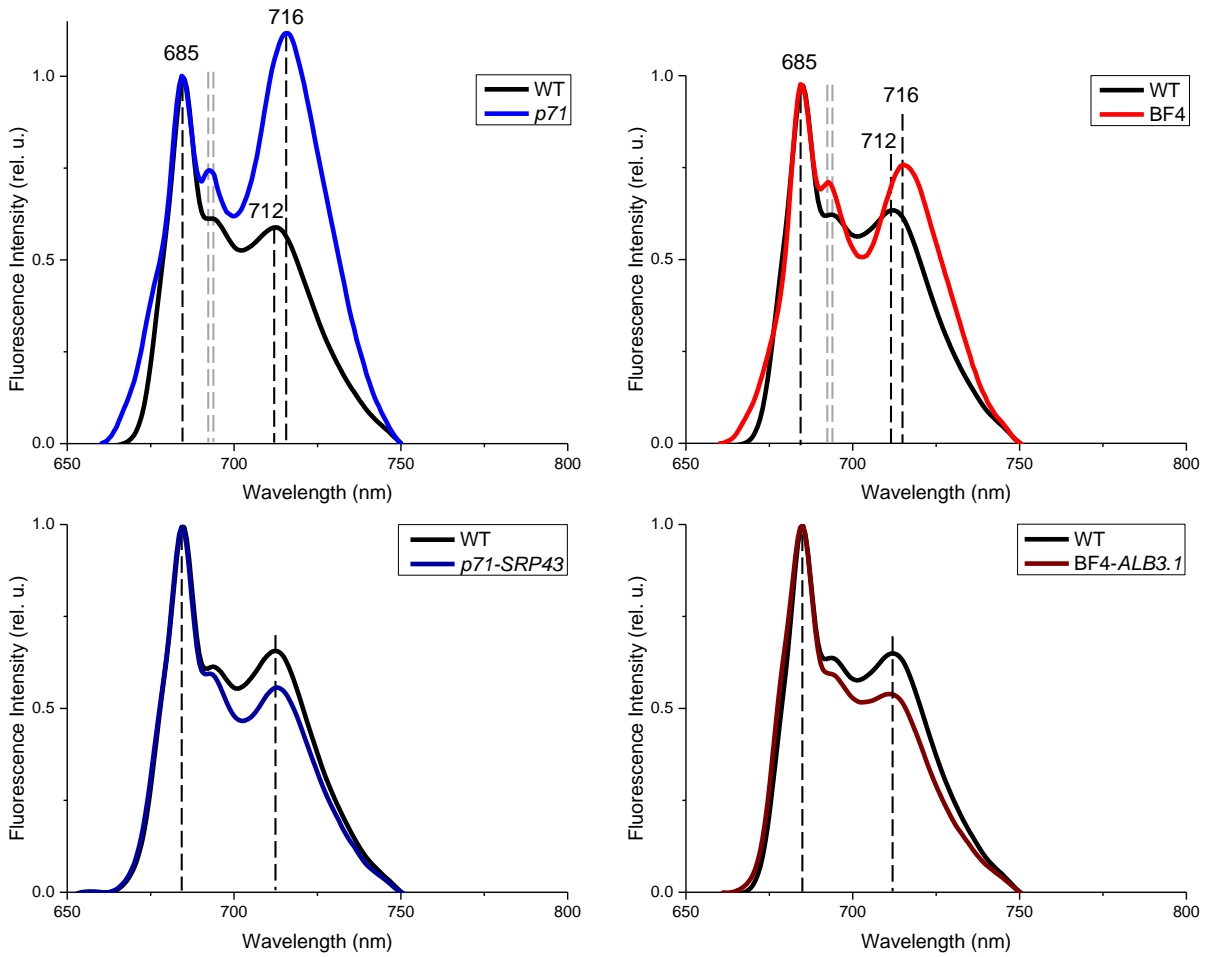


Figure 4: Low-temperature (77K) fluorescence emission spectra of cells in state 1 of wild type (WT), light-harvesting complex mutants (*p71* and BF4) and the complemented mutants grown in moderate light ($50 \mu\text{mol photons m}^{-2} \text{s}^{-1}$). All fluorescence emission spectra are normalized on PSII emission at 685 nm.

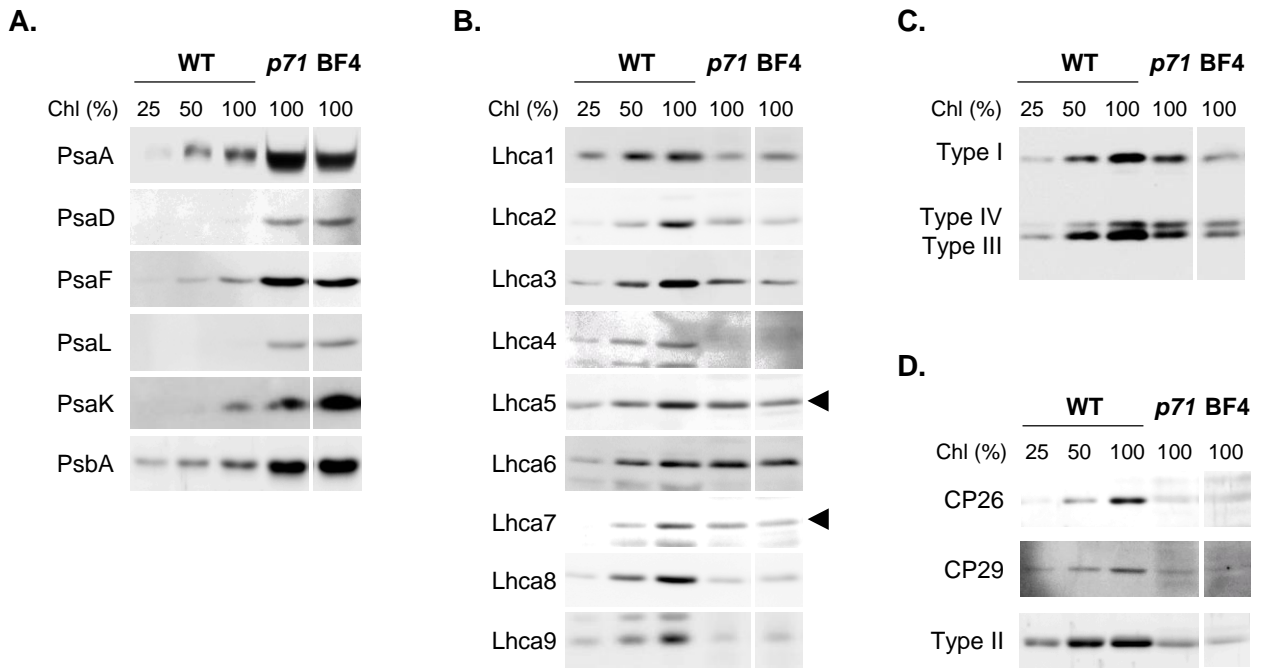


Figure 5: Accumulations of PSI, PSII, LHCI, and LHCII proteins in *p71*, BF4 and wild type, on a chlorophyll basis. WT (wild type), *p71* and BF4 cells were grown in TAP medium, and resuspended in buffer (50 mM Tris HCl pH 8.0, 20% (w/v) glycerol, 1 mM EDTA-NaOH pH 8.0). Cells at 0.1 (C) or 0.2 μ g (A, B, and D) Chls were solubilized with 2% (w/v) SDS and 0.1 M DTT at 100°C for 1 min, and protein extracts were separated by SDS-PAGE, electroblotted onto a nitrocellulose filter, probed with specific antibodies, and visualized by enhanced chemiluminescence. The filter was hybridized with antibodies against (A) PSI and PSII proteins (PsaA, PsaD, PsaF, PsaL, PsaK and PsbA), (B) LHCI proteins (Lhca1-9), (C) LHCII proteins (Type I, III, and IV) (D) LHCII proteins (CP26, CP29, and LHCII Type II). The arrowheads indicate the signals representing the actual antigen.

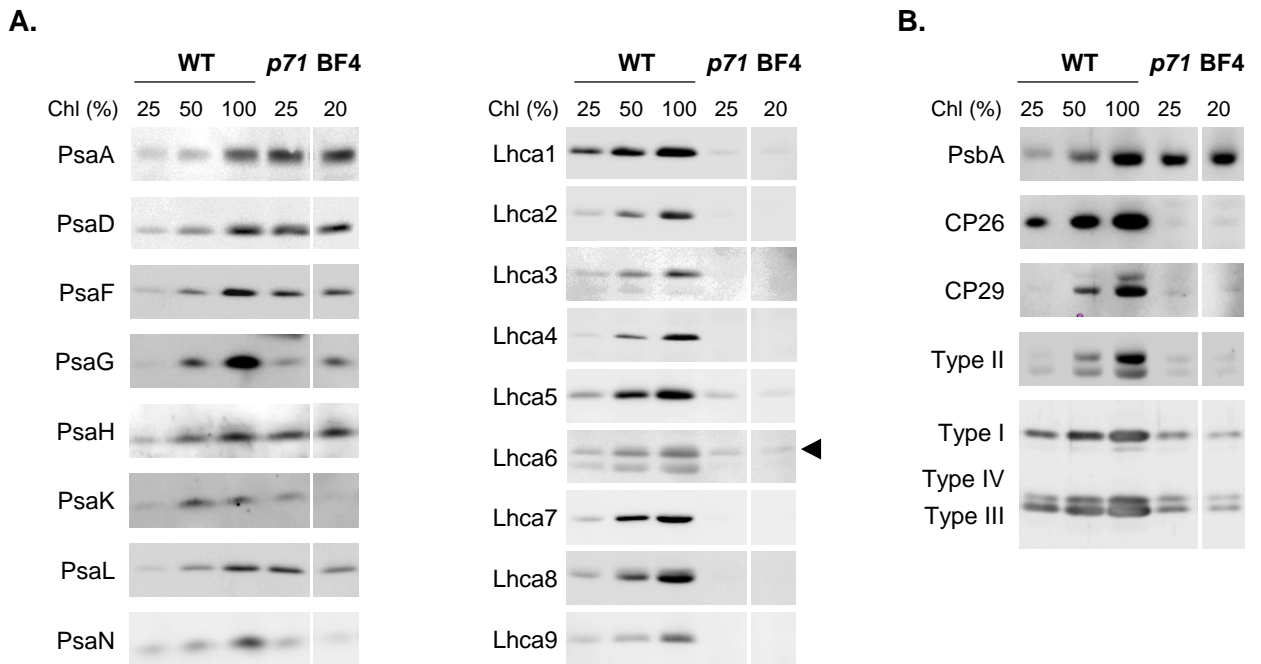


Figure 6: Accumulations of LHCI and LHCII proteins in *p71*, BF4 and wild type, on a reaction center basis. Cells were grown in TAP medium and resuspended in buffer (50 mM Tris HCl pH 8.0, 20% (w/v) glycerol, 1 mM EDTA-NaOH pH 8.0). Cells were solubilized with 2% (w/v) SDS and 0.1 M DTT at 100°C for 1 min, and protein extracts were separated by SDS-PAGE, electroblotted onto a nitrocellulose filter, probed with specific antibodies, and visualized by enhanced chemiluminescence. WT, wild type. The arrowhead indicates Lhca6. (A) Accumulation of PSI subunits and LHCI proteins on a PsaA basis. The nitrocellulose filter was hybridized with antibodies against PSI subunits (PsaA, PsaD, PsaF, PsaG, PsaH, PsaK, PsaL, and PsaN), LHCI (Lhca1-9). Relative loaded Chl amounts (%) are indicated on the top of lanes. (B) Accumulation of LHCII proteins on a PSII basis. The nitrocellulose filter was hybridized with antibodies against PSII (PsbA) and LHCII (CP26, CP29, LHCII Types I-IV). Relative loaded Chl amounts (%) are indicated on the top of lanes.

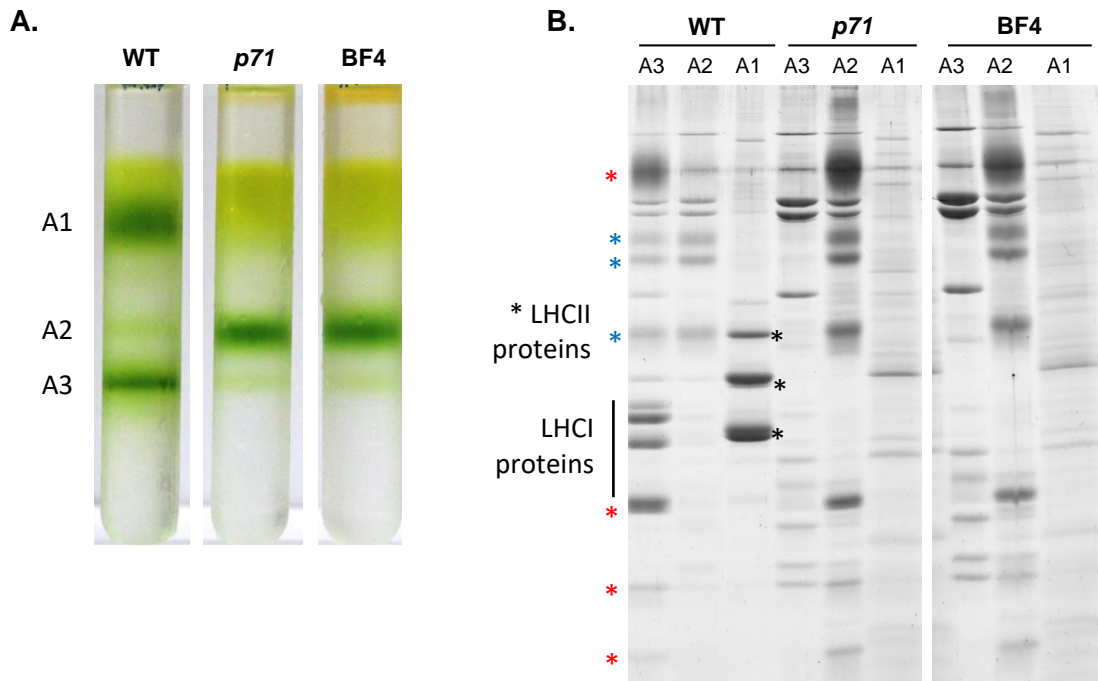
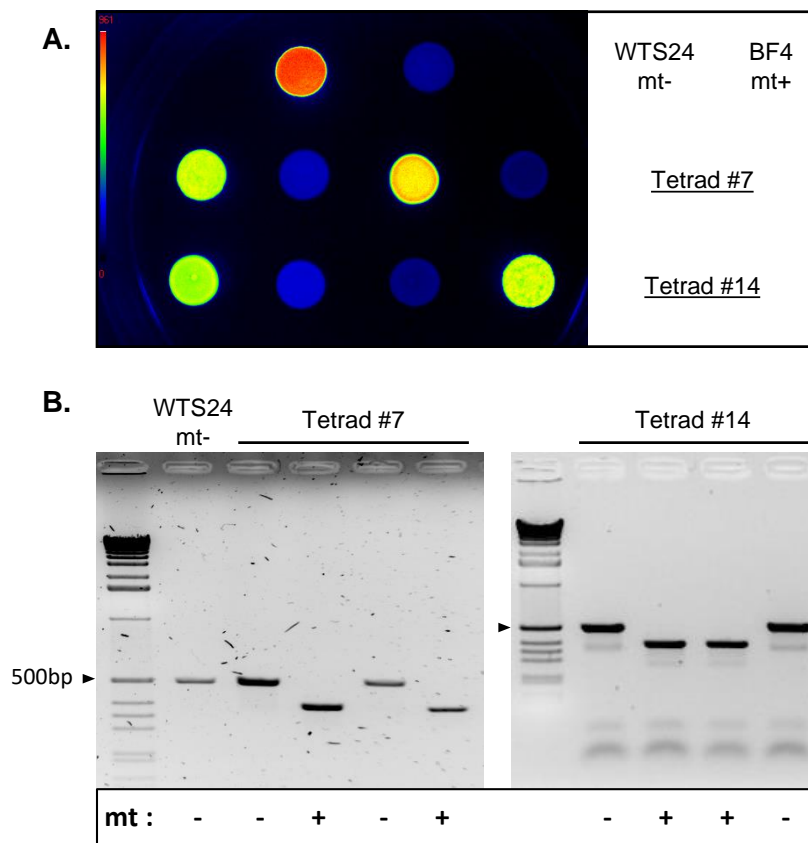
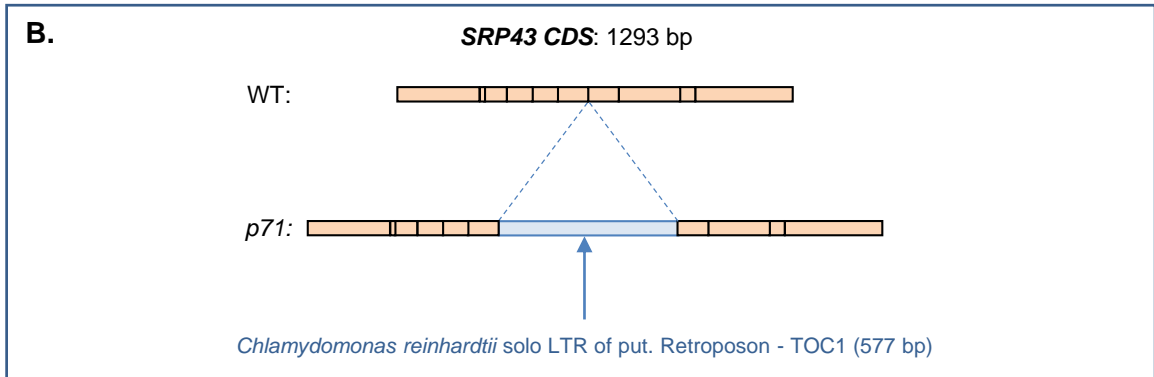
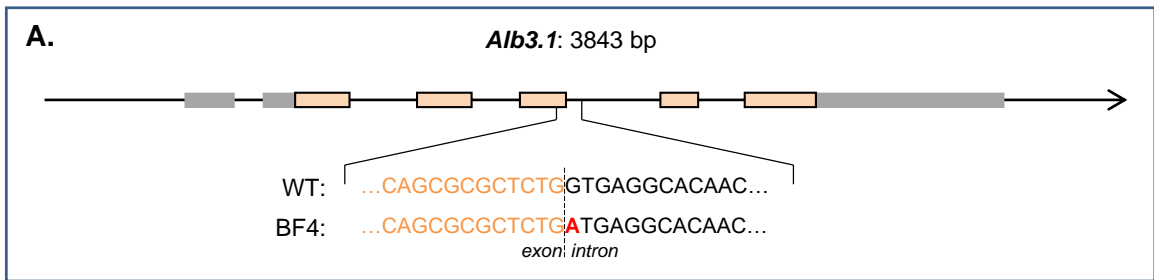


Figure 7: Separation of PSI, PSII, and LHCII complexes. (A) Thylakoid membranes of WT (wild type), *p71* and BF4 cells were solubilized with 0.8 % β -DDM and the extracts were separated by sucrose density gradient ultracentrifugation. A1, A2, and A3 represent LHCII, PSII core, and PSI-LHCI supercomplexes. (B) Polypeptides of A1, A2, and A3 were separated by SDS-PAGE and stained by Coomassie Brilliant Blue. Black asterisks: LHCII proteins, red asterisks: PSI proteins, and blue asterisks: PSII proteins.

Supplementary material

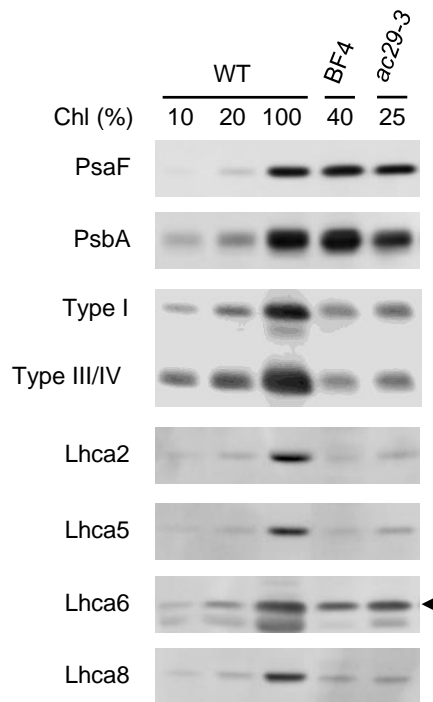


Supplementary Figure 1: Fluorescence (F_M) image (A) and PCR mating type test (B) of 2 typical tetrads from a cross between WTS24, mt- and BF4, mt+. Note that the BF4 progeny which are blue spots in (A) are mt+ in (B).



Supplementary Figure 2:

- (A) Genomic sequence of the *Alb3.1* gene in WT and BF4
- (B) The *SRP43* coding sequence (CDS) in WT and *p71*



Supplementary Figure 3: Comparative analysis of antenna protein content in BF4 and *ac29-3* mutants.

WT (wild type), BF4, and *ac29-3* cells were grown in TAP medium and cells were suspended in buffer (50 mM Tris HCl pH 8.0, 20% (w/v) glycerol, 1 mM EDTA-NaOH pH 8.0). Cells were solubilized with 2% (w/v) SDS and 0.1 M DTT at 100°C for 1 min. Cell proteins were separated by SDS-PAGE on a PSI basis, electroblotted onto a nitrocellulose filter, probed with specific antibodies, and visualized by enhanced chemiluminescence. The arrowheads indicate the signals representing the actual proteins. The filter was hybridized with antibodies against PsaF, PsbA, LHCII Type I, III, and IV, Lhca2, Lhca5, Lhca6, and Lhca8. Relative loaded amount of chlorophylls (%) are indicated on the top of blots.

Chlamydomonas reinhardtii - L18_domain

L18		VDPLYPGGS-FDPLGLADD	18
Lhca1		GGVV YPGGA-FDPLGFAKD	18
Lhca2		GETGFLSFAP FDPMGMKSE	19
Lhca3		GDAAY PGGP-FFNLFNLGK	18
Lhca4		NE PGYPGGI-FDPFGWSKG	18
Lhca5		PEMG YPGGI-FDPFGFSKG	18
Lhca6		HEVG YPGGV-FAPFIPGDL	18
Lhca7		LENG YPGGRF-FDPMGLSRG	19
Lhca8		SELG YPGGP-FDPLGLSKE	18
Lhca9		GTSGFINS FPFDPA GMNSP	19
Lhcb4	CP29	EKRC YPGGV-FDPLKLASE	18
Lhcb5	CP26	LDPLYPGGP-FDPLGLADD	18
LhcbM3	Type I	LDPLYPGES-FDPLGLADD	18
LhcbM4	Type I	LDPLYPGES-FDPLGLADD	18
LhcbM6	Type I	LDPLYPGES-FDPLGLADD	18
LhcbM8	Type I	LDPLYPGES-FDPLGLADD	18
LhcbM9	Type I	LDPLYPGES-FDPLGLADD	18
LhcbM5	Type II	LDKL H PGGQ F FDPLGLAED	19
LhcbM2	Type III	LDPL H PGGA- FDPLGLADD	18
LhcbM7	Type III	LDPL H PGGA- FDPLGLADD	18
LhcbM1	Type IV	LDK L YPGG S - FDPLGLADD	18
LhcSR1		KD D YE P GD L GF FDPLGL KPT	19
LhcSR3		KD D YE P GD L GF FDPLGL KPT	19

Supplementary Figure 4: Sequence alignment of L18 domain between LHCP proteins from *Chlamydomonas reinhardtii*. Conserved L18 domain is highlighted in blue and the DPLG motif in red.

parameter	WT	<i>srp43</i> mutants		<i>alb3.1</i> mutants		Complemented strains		
		<i>p71</i>	<i>tla3</i>	BF4	<i>ac29-3</i>	<i>p71-SRP43</i>	BF4-ALB3.1	
[Chl] ($\mu\text{g}/10^6$ cell)	DL	1.3 \pm 0.3	0.24 \pm 0.07	-	0.28 \pm 0.05	-	1.1 \pm 0.1	1.01 \pm 0.04
	ML	2.1 \pm 0.3	0.35 \pm 0.02	0.96 \pm 0.05	0.24 \pm 0.03	0.37 \pm 0.06	0.8 \pm 0.04	1.0 \pm 0.1
Chl <i>a</i> / Chl <i>b</i>	DL	2.9 \pm 0.2	8.2 \pm 0.2	-	8.4 \pm 0.8	-	3.2 \pm 0.1	3.5 \pm 0.1
	ML	3.1 \pm 0.1	6.9 \pm 0.4	6.2 \pm 0.1	9 \pm 2	12.7 \pm 0.3	4.1 \pm 0.2	3.2 \pm 0.1
F_M / Cell	DL	100%	8% \pm 3	-	8.1% \pm 0.5	-	71% \pm 2	79% \pm 3
	ML	100%	6.9% \pm 0.3	33.1% \pm 0.4	5% \pm 1	7.5% \pm 0.2	58% \pm 2	62% \pm 5
F_V / F_M	DL	0.75 \pm 0.01	0.35 \pm 0.02	-	0.35 \pm 0.06	-	0.70 \pm 0.01	0.68 \pm 0.04
	ML	0.74 \pm 0.02	0.33 \pm 0.03	0.52 \pm 0.01	0.35 \pm 0.01	0.31 \pm 0.02	0.74 \pm 0.01	0.64 \pm 0.06

Table 1: Chlorophyll content and fluorescence parameters of wild type (WT), *srp43* and *alb3.1* mutants and *p71-SRP43* and BF4-ALB3.1 complemented mutants. Chlorophyll concentrations were determined according to Porra *et al.* (1989). Percentage was determined by comparison of the mutant with the wild type cells grown under the same light condition. Values represent means \pm SD (n= 3 – 7). DL, dim light (5 $\mu\text{mol photons m}^{-2} \text{s}^{-1}$); ML, moderate light (50 $\mu\text{mol photons m}^{-2} \text{s}^{-1}$).